HGG Advances

REPORT

Biallelic variants in *MESD*, which encodes a WNT-signaling-related protein, in four new families with recessively inherited osteogenesis imperfecta

Thao T. Tran,[1,13] Rachel B. Keller,[2,13,14] Brecht Guillemyn,[3,13] Melanie Pepin,[2] Jane E. Corteville,[4] Samir Khatib,[5] Mohammad-Sadegh Fallah,[6] Sirous Zeinali,[6,7] Fransiska Malfait,[3] Sofie Symoens,[3] Paul Coucke,[3] Peter Witters,[8] Elena Levtchenko,[9] Hamideh Bagherian,[5,6] Deborah A. Nickerson,[10] Michael J. Bamshad,[10,11] Jessica X. Chong,[11] University of Washington Center for Mendelian Genomics, and Peter H. Byers[1,12,*]

Summary

The bone disorder osteogenesis imperfecta (OI) is genetically heterogeneous. Most affected individuals have an autosomal dominant disorder caused by heterozygous variants in either of the type I collagen genes (*COL1A1* or *COL1A2*). To date, two reports have linked Mesoderm Development LRP Chaperone (*MESD*) to autosomal recessive OI type XX. Four different biallelic pathogenic variants in *MESD* were shown to cause a progressively deforming phenotype, associated with recurrent fractures and oligodontia in five individuals in five families. Recently, compound heterozygosity for a frameshift predicted to lead to a premature termination codon in exon 2 of the 3-exon gene and a second frameshift in the terminal exon in *MESD* were detected in three stillbirths in one family with severe OI consistent with the neonatal lethal phenotype. We have identified four additional individuals from four independent families with biallelic variants in *MESD*: the earlier reported c.632dupA (p.Lys212Glufs*19) and c.676C>T (p.Arg226*)—which are associated with a severe form of OI—and one new pathogenic variant, c.603-606delTAAA (p.Asn201Lysfs*15), which causes a neonatal lethal form of OI. MESD acts in the WNT signaling pathway, where it is thought to play a role in the folding of the WNT co-receptors low-density lipoprotein receptor-related proteins 5 and 6 (LRP5/LRP6) and in chaperoning their transit to the cell surface. Our report broadens the phenotypic and genetic spectrum of *MESD*-related OI, provides additional insight into the pathogenic pathways, and underscores the necessity of MESD for normal WNT signaling in bone formation.

Osteogenesis imperfecta (OI [MIM: 166200, 166210, 259420, 166220]; see Table S1 for full list of genes) is a heritable bone dysplasia characterized by low bone mass and fragile bones with fractures—hence, the commonly used description "brittle bone disease." The vast majority of OI individuals harbor a heterozygous pathogenic variant in one of the two genes that encode the chains of type I procollagen (*COL1A1* [MIM: 12050], *COL1A2* [MIM: 120160]), the precursor of the major protein of bone.[1] In the last 15 years, genetic studies have expanded our understanding of the causative mechanisms that underlie OI. It is now appreciated that rare recessive forms of OI result from variants in almost two dozen genes that encode proteins involved in regulation of collagen production; assembly, transport, chaperoning, and secretion of collagens; extracellular processing of collagen; and regulation of signaling pathways.[2] One of these is the Wingless-related integration site (WNT) signaling pathway, whose involvement in bone biology has not been fully elucidated. Variants in *WNT1* have been linked to severe OI (MIM: 615220) and to osteoporosis,[3–6] and targets of WNTs that are important for bone development and homeostasis are thought to include alkaline phosphatase (*ALPL* [MIM: 171760]), which plays a role in bone mineralization, and Specificity Protein 7 (*SP7* [MIM: 606633]), which encodes a transcription factor that controls preosteoblast-to-osteoblast transition.[7,8] Variants in *ALPL* cause hypophosphatasia (MIM: 146300 and 241510),[9] and two reports associate *SP7* with a recessive form of OI (MIM: 613849).[10,11]

MESD (MIM: 607783), previously called *MESDC2*, encodes the endoplasmic reticulum (ER) resident chaperone protein MESD (Mesoderm development candidate 2) and consists of a signal sequence (residues 1–33), a chaperone domain (residues 34–164), an escort domain (residues

[1]Department of Laboratory Medicine and Pathology, University of Washington, Seattle, WA 98195, USA; [2]Department of Pathology, University of Washington, Seattle, WA 98195, USA; [3]Center for Medical Genetics Ghent, Ghent University Hospital, Department of Biomolecular Medicine, Ghent, Belgium; [4]Department of Reproductive Biology, Case Western Reserve University, Cleveland, OH 44106, USA; [5]GMDC Al Quds University, P.O. Box 5100, Abu Dis, Palestine; [6]Department of Medical Genetics, Kawsar Human Genetics Research Center, Tehran, Iran; [7]Department of Molecular Medicine, Biotechnology Research Center, Pasteur Institute of Iran, Tehran, Iran; [8]Center for Metabolic Diseases, University Hospital Leuven, Department of Paediatric Gastroenterology, Hepatology, and Nutrition, Leuven, Belgium; [9]University Hospital Leuven, Departments of Pediatric Nephrology and Development and Regeneration, Leuven, Belgium; [10]Department of Genome Sciences, University of Washington, Seattle, WA 98195, USA; [11]Department of Pediatrics, University of Washington, Seattle, WA 98195, USA; [12]Department of Medicine (Medical Genetics), University of Washington, Seattle, WA 98195, USA
[13]These authors contributed equally
[14]Present address: Division of Gastrointestinal Cancers, Department of Medical Oncology, Dana-Farber Cancer Institute and Harvard Medical School, Boston, MA, 02115 USA
*Correspondence: pbyers@uw.edu
https://doi.org/10.1016/j.xhgg.2021.100051.

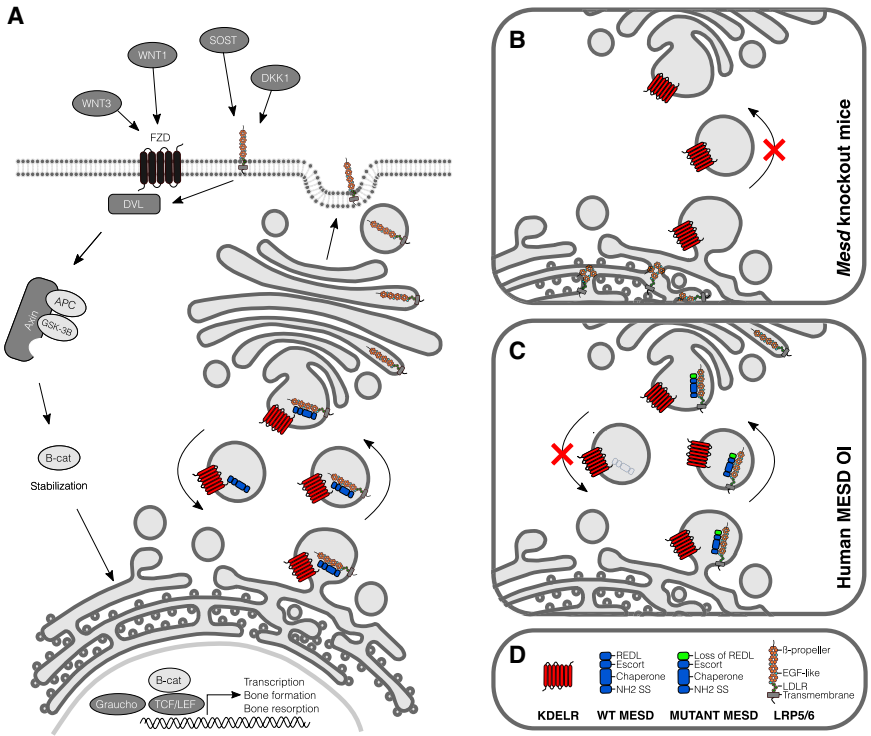

Figure 1. Function and location of MESD in the WNT signaling pathway (in bone cells)

(A) Canonical WNT signaling involves binding of WNT proteins to the frizzled receptor (FZD) and to the co-receptors LRP5 and LRP6. Formation of this complex leads to the inhibition of glycogen synthase kinase 3β (GSK-3β), which phosphorylates β-catenin. Unphosphorylated β-catenin is safeguarded from proteosomal degradation, accumulates, and moves into the nucleus where it triggers lymphoid enhancer factor (LEF)/T cell factor (TCF)-mediated gene transcription.[13] MESD is thought to play a role in the folding of the WNT co-receptors LRP5 and LRP6 and in chaperoning their transit to the cell surface; the C-terminal REDL ER-retention sequence of MESD allows for retrieval from the Golgi.

(B and C) Close-up views of aberrant MESD signaling in mice and humans. LRP5/6 do not fold properly in *Mesd* knockout mice and appear to aggregate in the RER (B). We hypothesize that the mutant MESD proteins described in this report have (residual) chaperone activity to signal LRP5/6 to the cell surface but fail for retrieval from the Golgi since they lack the REDL sequence (C). This leads to disturbed WNT signaling in bone (LRP5) and tooth development (LRP6).

(D) Legend of most important protein structures in MESD-related WNT signaling: KDELR receptor, red; wild-type (WT) and mutant MESD proteins with/loss of REDL, blue/green; LRP5/6, gray/green/cyan/orange.

165–204), and a COOH-terminal KDEL-like sequence (REDL) that distinguishes it from the secreted proteins it chaperones and allows for retrieval from the Golgi.[12] The protein facilitates folding of the β-propeller domains of two WNT co-receptors, low-density lipoprotein receptor-related protein 5 and 6 (LRP5/LRP6), and in their localization to the cell surface (Figures 1, 2 A, and 2B).[16] LRP5 regulates peak bone mass in vertebrates, and homozygosity for inactivating variants in *LRP5* causes osteoporosis-pseudoglioma syndrome (OPPG; MIM: 259770),[17] whereas *LRP5* gain-of-function variants are implicated in high bone mass (HBM) phenotypes that include endosteal hyperostosis (MIM: 144750), van Buchem disease (MIM: 607636), and osteopetrosis (MIM: 607634).[18–20] In addition, *LRP6* loss-of-function variants resulted in altered glycosylation and abrogated activation of the WNT signaling pathway, contributing to the etiology of non-syndromic autosomal dominant oligodontia.[21] Homozygous *Mesdc2* knockout mice fail to establish a primitive streak and lack a developed mesoderm[22] due to a patterning defect in the proximal epiblast.[16] This patterning defect is similar to the outcome when another WNT family member, *Wnt3*, is knocked out in embryos.[23]

Biallelic pathogenic variants, all located in the final (third) exon, in *MESD* were recently identified in five individuals from five families who presented with moderately severe, progressively deforming recessive OI, which one individual had with oligodontia.[14] With overexpression studies in HEK293T cells, Moosa et al.[14] suggested that the OI-associated *MESD* mutations produced hypomorphic alleles whose failure to remain within the ER was significantly reduced but did not completely eliminate LRP5 and LRP6 trafficking. Recently, infants from one family who harbored compound heterozygous frameshift variants, one that resulted in the premature termination codon in exon two and the other a premature termination in exon three, had a lethal OI picture, similar to OI type II caused by type I collagen gene pathogenic variants. Histological analysis of femoral, calvarial, and spinal bone revealed impaired osseous development with altered osteocyte morphology and reduced canalicular connectivity. Bone mineral density distribution measured by quantitative backscattered electron imaging indicated impaired and more heterogeneous matrix mineralization in the described MESD fetuses than in controls.[15] OI that results from pathogenic variants in *MESD* has been designated as OI type XX (MIM: 618644) in OMIM. Here, we present four new *MESD* individuals and used fibroblast studies to get additional insight into the pathogenic pathways of the *MESD*-related OI subtype.

We used whole-exome sequence analysis (WES) to study an infant from a consanguineous family in which we had not previously identified a causative variant in targeted OI-related gene sequences. We identified a homozygous likely pathogenic variant in *MESD* in the affected proband

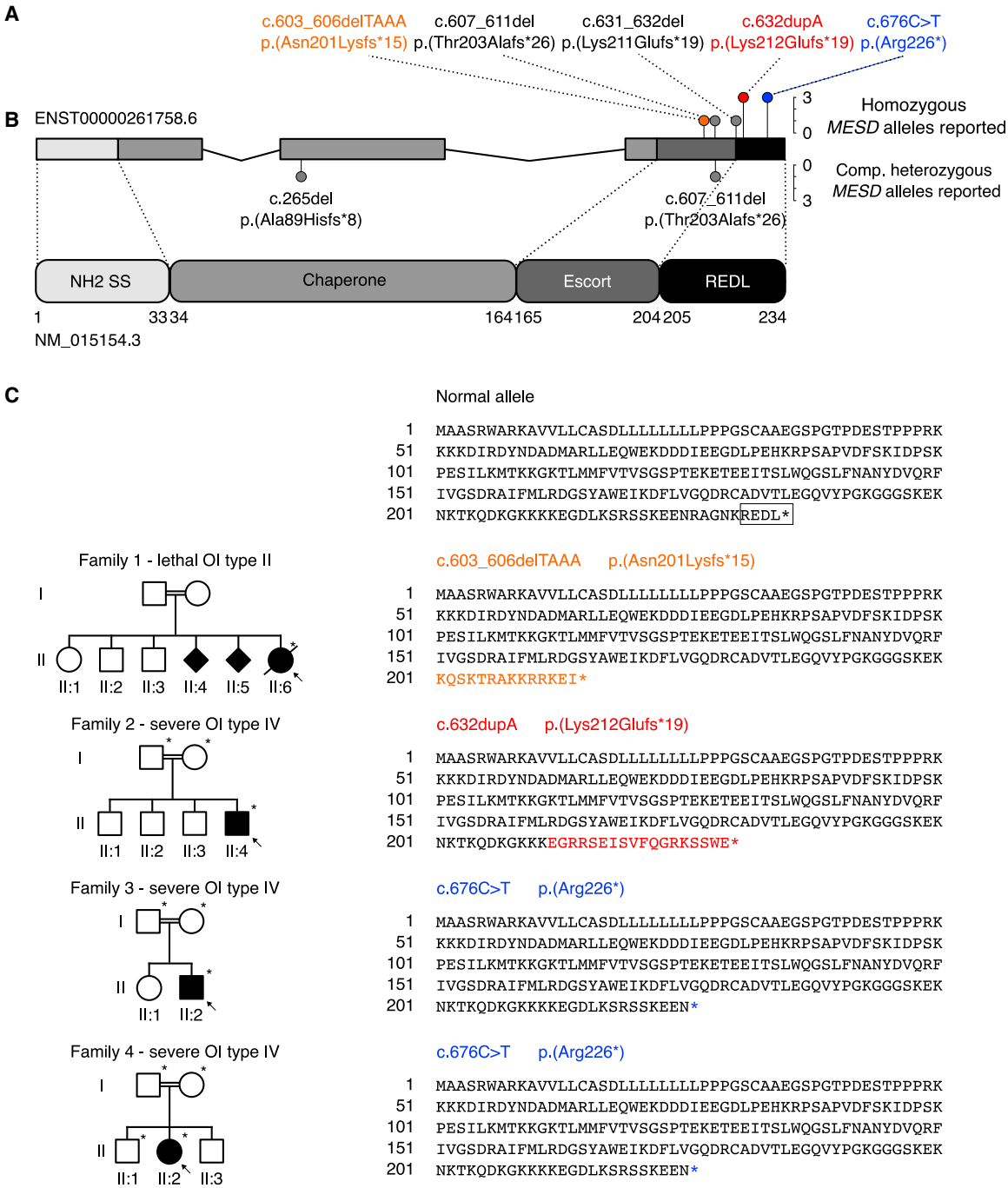

Figure 2. Structure of the *MESD* gene and MESD protein, pedigrees of the described families, and representation of the mutant allele sequences

(A) The *MESD* gene consists of 3 exons (4,200 bp) and comprises 14.07 kb on chromosome 15. The cumulative frequency of the six known pathogenic *MESD* alleles (both this and two previous studies[14,15]) are denoted with colored lollipop graphs. The pathogenic alleles included in this report are highlighted in orange, red, and blue, respectively.

(B) Full-length MESD protein consists of 234 amino acids (aa) and contains 4 functional domains.

(C) Pedigrees of the 4 families with *MESD* variants and representation of the WT and mutant alleles. The proband in each family is indicated by an arrow. Filled circles, squares, or diamond structures represent individuals with OI. Individuals who were studied in each family are noted with asterisks. The variants in families 1 and 2 cause frameshifts and introduce premature termination codons 15 and 19 codons downstream of the frameshifts, respectively, and the variant in families 3 and 4 changes an asparagine residue to a stop codon, resulting in premature termination. All three variants cause the loss of the C-terminal REDL ER-retention sequence (marked with a square in the WT allele) needed for retrieval from the Golgi, and their position and mutant AA sequence is highlighted in orange, red and blue, respectively (matching colors in A).

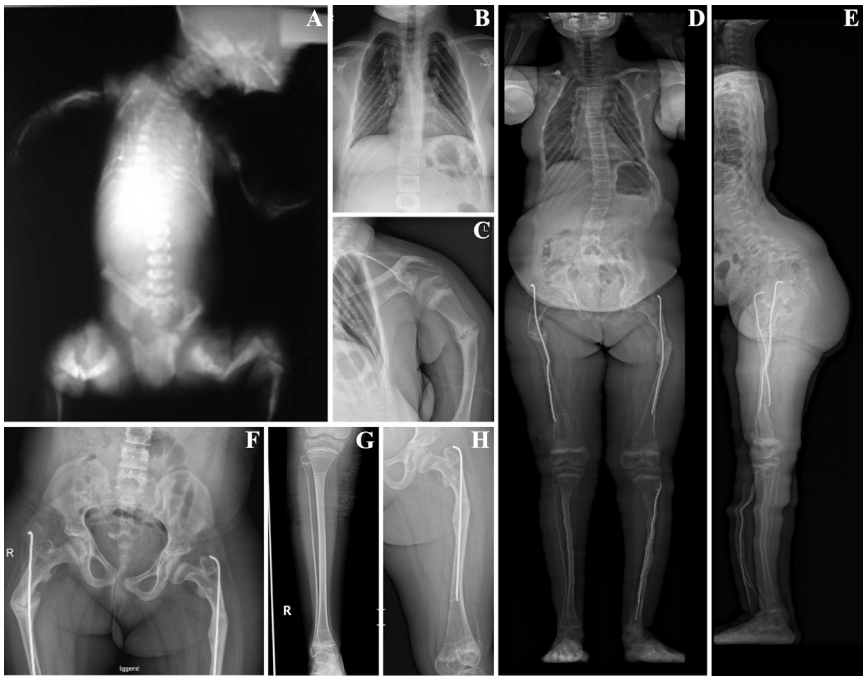

Figure 3. Clinical spectrum of *MESD* pathogenic variants

(A) Imaging of individual P1-II:6 shows limited calvarial mineralization, a small chest with thin ribs, fractures in upper and lower extremities, and platyspondyly. (B–H) Individual P4-II:2 presents with scoliosis (D and E), mild bowing of upper and lower limbs (C–H), fracture of the left humerus (C), and (bilateral) post-surgical rodding of the lower leg (D) and femoral shafts (D, E, F, and H), respectively. The impact of bisphosphonate treatment can be noted in the right lower (G) and left upper leg (H).

Clinical pictures/radiographs taken in the neonatal period (A) or at the age of 11 (B and C) and 12 years (D–H), respectively.

(c.603-606delTAAA [p.Asn201Lysfs*15] in family 1, individual 1-II:6, described later). We subsequently identified homozygous variants in three additional independent OI probands, two by means of targeted Sanger sequencing of *MESD* analysis (c.632dupA [p.Lys212Glufs*19] and c.676C>T [p.Arg226*] in families 2 and 3, respectively) and in family 4 by clinical whole exome analysis.

The proband from family 1 (1-II:6; Figure 3A) died in the neonatal period. She had a small chest and multiple fractures. Radiographs showed a thin calvarial mantle, thin deformed ribs with multiple fractures, and short long bones (Figure 3A). The radiographic features were consistent with severe OI (type III).[6] No other clinical information was available. Her parents (1-I:1 and 1-I:2) were double first cousins. They had two prior pregnancies that were also affected (1-II:4 and 1-II:5) and had three unaffected children (1-II:1, 1-II:2, and 1-II:3). To identify the causative gene in this family (Figure 2C), we used the same WES dataset previously described by Pyott et al.[3] A detailed methodology on the exome filtering is provided in the Supplemental methods (Exome filtering). Of the candidate genes that were identified using this approach, none had known clinical implications relating to skeletal disorders, but one gene, *MESD* (Figure 2A), was involved in a pathway known to be important to bone development. Individual 1:II-6 was homozygous for a 4-bp deletion in the last exon of *MESD* (c.603-606delTAAA [p.Asn201Lysfs*15]) that was predicted to lead to a frameshift and premature termination within the exon (Figure 2C). Sequence analysis of cDNA from the proband's cultured skin fibroblasts showed that all stable transcripts had the deletion (Figure S1). Analysis of collagen synthesized and secreted by the proband's cultured dermal fibroblasts revealed no alterations in the electrophoretic mobility of the chains of type I procollagen or in the efficiency of secretion (data not shown). Parental samples were not available to confirm that each carried the variant or to determine if the deletion-bearing transcript was as stable as that encoded by the normal allele.

The proband from family 2 (2-II:4) was a 5-year-old boy who had been diagnosed with OI at birth as a result of multiple in utero fractures. When assessed at the age of 5 years, he had a triangular facial shape, lower limb and shoulder deformities, and poor muscle tone. He was non-ambulatory. Most of his teeth had fallen out, but it was unclear whether this was due to dentinogenesis imperfecta (DI), clinical oligodontia (in accordance to previously reported MESD individuals[14]), or other factors (e.g., poor nutrition, gum disease). His parents (2-I:1 and 2-I:2) were first cousins. Sanger sequencing of *MESD* revealed a homozygous single base pair duplication in the last exon (c.632dupA [p.Lys212Glufs*19]) that led to a frameshift and a premature termination in the same exon (Figures 2A and 2C). His parents were each heterozygous for the duplication (Figure S1). Cultured fibroblasts were not available from the proband or from the parents.

The proband in family 3 (3-II:2) was a 5-year-old boy with blue sclerae; multiple fractures in his upper and lower limbs, sternum, and ribs; and deformities of his left femoral and right upper limb following femoral shaft osteotomy and fixation. His parents (3-I:1 and 3-I:2) were first cousins once-removed. The boy was homozygous for a pathogenic nonsense variant in *MESD* (c.676C>T [p.Arg226*]) that deletes the last 9 amino acids of the protein (Figures 2A and 2C). His father and mother were each carriers of the pathogenic variant (Figure S1). No fibroblasts were available from the proband.

The 12-year-old proband from family 4 (4-II:2) was the middle child of consanguineous parents of Palestinian origin. She has two healthy brothers and had presented to medical care at age 10 months with a history of multiple

Table 1. Cumulative overview of molecular, clinical, and radiographic findings of the autosomal recessive *MESD* individuals reported to date

Findings	Cumulative numbers (12 individuals)
Location of pathogenic *MESD* alleles	homozygous in last exon (3): 9/12; compound heterozygous in exon 2 and 3: 3/12
Gender	4 females, 8 males
Consanguinity	9/12
Bisphosphonate treatment	5 have a history of bisphosphonate treatment
Confirmed prenatal fractures	7/12
Color of sclera	5 bluish, 3 white, 4 N/A
Disorganized dentition/clinical oligodontia	3 yes, 1 no, 1?, 7 N/A
Hearing impairment	3 no, 1 yes, 8 N/A
History of fractures	12/12
Vertebral/thoracic cage/rib fractures	11 yes, 1 no
Retarded gross motor function	6 yes

Findings for eight of the individuals were previously published (Moosa et al.[14] and Stürznickel et al.[15]), and four are presented in this report. N/A, not available.

low-impact fractures, severe osteoporosis (T- and Z-scores of −7.3 and −5.9), mild bowing of the upper and lower limbs, generalized muscle hypotonia, and severe hyperlaxity of the small joints. She had soft and somewhat translucent skin, had mildly dilated post-operative scars, and did not present with DI. She had severe psychomotor retardation (likely to be caused by the identified variant), polycystic kidney disease (inherited from her mother's side), and a history of Langerhans cell histiocytosis. Pamidronate treatment was discontinued because of very little improvement, but zoledronate administration led to higher bone mineral content. She had Ilizarov surgery, and at age 3 years, she remained mostly nonambulatory. A detailed overview of the radiological features of this individual is highlighted in Figures 3B–3H. Karyotype of the proband in this family was normal, and whole-genome array comparative genomic hybridization (180k Agilent Array) did not reveal any chromosomal deletions/duplications. No alterations in the electrophoretic migration pattern of the fibrillar collagens type I, III, and V were noted (data not shown). Molecular analysis by means of a clinical WES approach (similar filtering strategy as described in Guillemyn et al.[24]) revealed the same homozygous pathogenic variant in *MESD* as described in family 3 (c.676C>T [p.Arg226*]) (Figures 2A and 2C). Her father and mother were each carriers of the pathogenic variant, and one of her healthy brothers who was available for genetic testing did not carry the pathogenic variant (data not shown).

The four individuals reported here had OI phenotypes that ranged from moderately severe to lethal in the perinatal period and are similar in clinical presentation to the *MESD* individuals that were described by Moosa et al.[14] A cumulative overview of the molecular and salient clinical and radiographic findings of all 12 autosomal recessive *MESD* individuals reported to date is provided in Table 1: all individuals presented with a history of fractures (7/12 confirmed prenatal fractures), and homozygous or compound heterozygous frameshift variants were identified in all 12. Nine had a consanguineous background, five had blue sclerae, three presented with clinical oligodontia, only one had hearing impairment, and a delayed gross motor function was noted in half of the individuals reported to date (6/12).

The explanation for the variation in severity of the phenotypes is not yet apparent. The variants that we identified are not noted in the NHLBI Exome Variant Server (EVS), the ExAC database, gnomAD, or in dbSNP. In the gnomAD database, there are 8 heterozygous variants (12 individuals) that produce premature termination codons in the last exon that might have similar effects to those seen here. This represents a carrier frequency of about 1/10,000 individuals, meaning homozygosity or compound heterozygosity would lead to a very low frequency of the disorder in the population represented in those collections. *MESD* variants accounted for about 5% of the approximately 100 unsolved OI families we tested but represent only 4 of more than 3,500 OI individuals in whom we have identified the causative variants.

As also noted by Moosa et al.,[14] the three pathogenic variants that we identified were found in the last exon of *MESD*, as were the resulting premature termination codons. We could isolate and sequence cDNA from the cultured cells available from individual 1-II:6, thereby complementing the earlier observations of stable mRNA transcripts. Despite these, the MESD protein was not detected in the cell lysate from 1-II:6 fibroblasts, while it was detected in control cells (Figure 4A). To assess the relative stability of the mutant MESD proteins, we performed coupled *in vitro* transcription/translation (IVTT) for each of the variant sequences and found that the wild-type sequence and all the variant constructs produced stable MESD proteins (Figure 4B). Nonetheless, immunocytochemical studies of MESD in primary fibroblasts from 1-II:6 showed weak and diffuse staining compared to the strong ER-localized staining observed in control fibroblasts (Figure 4C). Cultured fibroblasts from 1-II:6 (family 1) had intracellular levels of LRP5 and LRP6 that were similar to control (Figure 4A), but we were unable to determine if those proteins tracked to the cell surface.

In all four families, the frameshift or stop-gain variants result in loss of the REDL sequence but retention of the chaperone and escort domains. It is possible that loss of the REDL signal results in MESD secretion rather than being recycled to the ER. Previous studies demonstrated that in HEK293T cells engineered to overexpress a mutant MESD protein that lacked the REDL sequence, MESD was not retrieved from the Golgi, and some traveled through the secretory pathway into the medium.[16] One limitation of those studies is that the gene was overexpressed, and

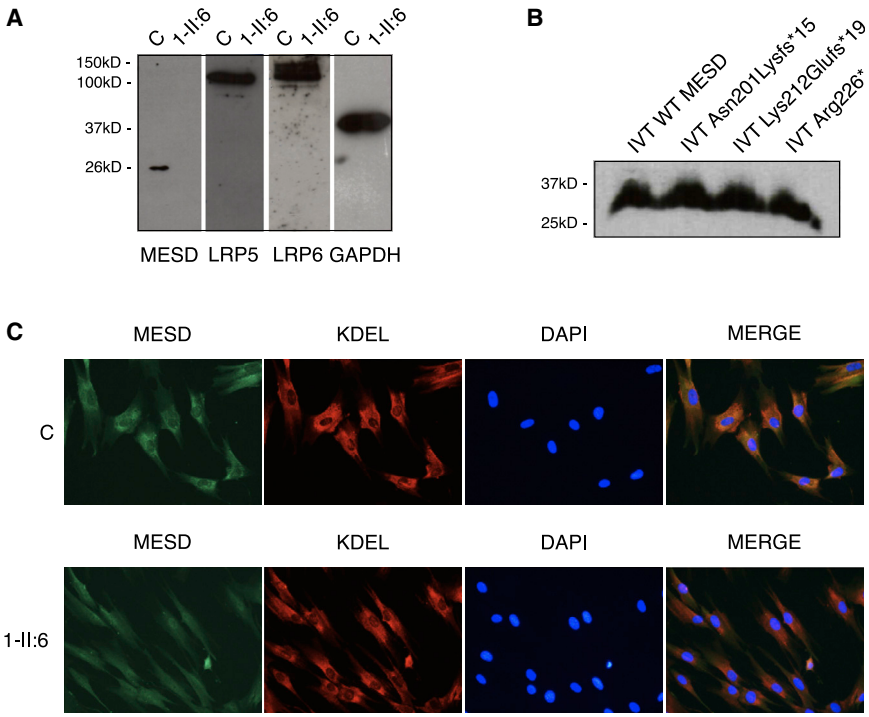

Figure 4. Loss of the REDL sequence in MESD is pathogenic

(A) Protein studies on cultured fibroblasts from the proband in family 1 (1-II:6) demonstrate the absence of MESD protein in the cell lysate. Levels of LRP5 and LRP6 appear normal. Images are of a single blot that was probed, washed, and re-probed for each of the targets (MESD, LRP5, LRP6, GAPDH). Western blot.

(B) IVTT of the variant *MESD* sequences results in production of stable MESD protein in all cases.

(C) Variant MESD lacking the REDL sequence is weakly staining and diffuse throughout the cytoplasm in 1-II:6 primary fibroblasts, while it is properly ER-localized in healthy control cells. Immunocytochemical.

saturation of available KDEL receptors would mean either that there was degradation or that some of the protein was contained in vesicles that proceeded from the rough endoplasmic reticulum (RER) to the Golgi and then to the cell surface. Alternatively, loss of the REDL sequence may destabilize the protein, a possibility suggested by study of other OI-causing genes involved in the collagen synthetic pathway. In the Prolyl-3 Hydroxylase (P3H1)-Cartilage-Associated Protein (CRTAP)-Cyclophilin B (CypB) molecular complex, responsible for the post-translational modification of type I collagen proα chains, if either the KDEL-containing P3H1 or the KDEL non-containing CRTAP is null, both proteins are unstable and absent from the cell.[25] It was later reported that loss of the P3H1 KDEL retention sequence alone was sufficient for loss of both P3H1 and CRTAP and the cause of OI in one family, though only intracellular P3H1 and CRTAP were analyzed, leaving open the question of whether stable secreted protein from these cells would be detectable.[26] While we were able to detect LRP5 and LRP6 protein in cell lysates from affected individuals' cells, we were not able to determine their localization using immunocytochemistry. This could have been due to poor cell quality. It is also unclear whether the expression and activity of MESD, LRP5, LRP6, and the appropriately interacting WNTs in fibroblasts are representative of osteogenic cells.

The range of the clinical presentations in individuals with biallelic pathogenic variants in *MESD* is striking, as it extends from a very severe peri- or prenatal lethal phenotype to one that fits into the more affected end of the original OI type IV range of Sillence (Moosa et al.,[14] Stürznickel et al.,[15] and this report). From these reports it is clear that heterozygosity, even for a likely null allele, is tolerated without clinical effect. Compound heterozygosity for a null and a frameshift premature termination codon in the last exon produces a very severe and lethal form of OI, similar to the severe OI type II picture. The mildest phenotype appears to result from a late premature termination codon that deletes the last 8 amino acids of the MESD protein, including the REDL sequence that permits recycling of the protein from the Golgi but retains the domains of the protein involved in the stabilization of the propeller motifs of the LRP proteins.

In the absence of MESD in knockout mice, LRP5 and LRP6 are retained in the ER as high-molecular-weight aggregates.[16] This appears to reflect the loss of proper folding in the propeller domains of the LRP proteins that is contributed by the chaperone function of MESD. MESD is vectorially inserted into the RER as a consequence of its amino terminal signal sequence. The carboxy-terminal RDEL sequence would then permit attachment to a KDEL receptor protein in the RER membrane. LRP5 and LRP6, both of which interact with MESD, are transmembrane proteins with the large, ultimately external facing domain in the RER lumen. These portions of the LRP proteins contain both the propeller domains and the LDL-like receptor domains that interact with frizzled proteins and WNT proteins on the cell surface. It seems likely that the loss of the REDL anchor would limit interaction of MESD with the membrane-anchored LRP proteins and so limit the correct folding of the propeller domains. The normal life cycle of MESD would be to facilitate incorporation of the two LRP proteins into RER vesicles that are then transported to the Golgi. Once there, they should dissociate and return to the RER, while the LRP proteins would continue to their cell surface localization. In the absence of MESD, both the chaperone and guidance to the Golgi functions would be lost. It appears, however, that all the mutations that we have encountered must facilitate LRP folding, after which at least some of the folded LRP proteins could negotiate transport to the Golgi and then on to the cell

surface without the MESD fellow traveler. The fate of the RDEL-lacking MESD remains uncertain. Overexpression studies show secretion into the culture medium, but this level of expression is likely to overwhelm the capture of the protein by the KDEL-receptor mechanisms. It is also not clear how LRP5 and/or LRP6 would be secreted, given their status as transmembrane-anchored proteins. In-depth investigation of fibroblast or osteogenic cells of MESD individuals, as well as animal models deficient for Mesd, Lrp5, and/or Lrp6, will be key to (1) study the exact role and fate of mutant MESD proteins, (2) shed light on the direct consequences on LRP5 and/or LRP6 secretion, and (3) define the respective roles of LRP5/6 in the development of bone and teeth phenotypes, respectively. In addition to these studies, the identification of more individuals with *MESD* defects, potentially including structural variants that disrupt different functional domains of the MESD protein, will further increase our understanding of the pathophysiological mechanism underlying this condition.

Supplemental information

Supplemental information can be found online at https://doi.org/10.1016/j.xhgg.2021.100051.

Acknowledgments

We thank the families for participating in this study. This work was supported by the Freudmann Research Fund at the University of Washington, the National Institute of Arthritis and Musculoskeletal and Skin Diseases (F31AR069971), the Cell & Molecular Biology Training Grant (5T32GM007270), the Molecular Medicine Training Grant (5T32GM095421), the UW Department of Pathology, the Collagen Diagnostic Laboratory, Ghent University (Methusalem grant 08/01M01108), and Research Foundation Flanders (1842318N to F.M.). Analysis assistance was provided by the University of Washington Center for Mendelian Genomics (UW-CMG) and was funded by the National Human Genome Research Institute and the National Heart, Lung, and Blood Institute grant HG006493 to D.A.N., M.J.B., and Suzanne Leal. The content is solely the responsibility of the authors and does not necessarily represent the official views of the National Institutes of Health.

Declaration of interests

M.J.B. is the Editor of Human Genetics and Genomics Advances. All other authors declare no competing interests.

Received: April 15, 2021
Accepted: August 13, 2021

Web resources

OMIM, https://www.omim.org
ExAC, http://exac.broadinstitute.org
EVS, https://evs.gs.washington.edu/EVS/
gnomAD, https://gnomad.broadinstitute.org/

References

1. Marini, J.C., Forlino, A., Cabral, W.A., Barnes, A.M., San Antonio, J.D., Milgrom, S., Hyland, J.C., Körkkö, J., Prockop, D.J., De Paepe, A., et al. (2007). Consortium for osteogenesis imperfecta mutations in the helical domain of type I collagen: regions rich in lethal mutations align with collagen binding sites for integrins and proteoglycans. Hum. Mutat. *28*, 209–221.
2. Marini, J.C., Forlino, A., Bächinger, H.P., Bishop, N.J., Byers, P.H., Paepe, A., Fassier, F., Fratzl-Zelman, N., Kozloff, K.M., Krakow, D., et al. (2017). Osteogenesis imperfecta. Nat. Rev. Dis. Primers *3*, 17052.
3. Pyott, S.M., Tran, T.T., Leistritz, D.F., Pepin, M.G., Mendelsohn, N.J., Temme, R.T., Fernandez, B.A., Elsayed, S.M., Elsobky, E., Verma, I., et al. (2013). WNT1 mutations in families affected by moderately severe and progressive recessive osteogenesis imperfecta. Am. J. Hum. Genet. *92*, 590–597.
4. Keupp, K., Beleggia, F., Kayserili, H., Barnes, A.M., Steiner, M., Semler, O., Fischer, B., Yigit, G., Janda, C.Y., Becker, J., et al. (2013). Mutations in WNT1 cause different forms of bone fragility. Am. J. Hum. Genet. *92*, 565–574.
5. Laine, C.M., Joeng, K.S., Campeau, P.M., Kiviranta, R., Tarkkonen, K., Grover, M., Lu, J.T., Pekkinen, M., Wessman, M., Heino, T.J., et al. (2013). WNT1 mutations in early-onset osteoporosis and osteogenesis imperfecta. N. Engl. J. Med. *368*, 1809–1816.
6. Fahiminiya, S., Majewski, J., Mort, J., Moffatt, P., Glorieux, F.H., and Rauch, F. (2013). Mutations in WNT1 are a cause of osteogenesis imperfecta. J. Med. Genet. *50*, 345–348.
7. Fujita, K., and Janz, S. (2007). Attenuation of WNT signaling by DKK-1 and -2 regulates BMP2-induced osteoblast differentiation and expression of OPG, RANKL and M-CSF. Mol. Cancer *6*, 71.
8. Heo, J.S., Lee, S.-Y., and Lee, J.-C. (2010). Wnt/β-catenin signaling enhances osteoblastogenic differentiation from human periodontal ligament fibroblasts. Mol. Cells *30*, 449–454.
9. Weiss, M.J., Cole, D.E., Ray, K., Whyte, M.P., Lafferty, M.A., Mulivor, R.A., and Harris, H. (1988). A missense mutation in the human liver/bone/kidney alkaline phosphatase gene causing a lethal form of hypophosphatasia. Proc. Natl. Acad. Sci. USA *85*, 7666–7669.
10. Lapunzina, P., Aglan, M., Temtamy, S., Caparrós-Martín, J.A., Valencia, M., Letón, R., Martínez-Glez, V., Elhossini, R., Amr, K., Vilaboa, N., and Ruiz-Perez, V.L. (2010). Identification of a frameshift mutation in Osterix in a patient with recessive osteogenesis imperfecta. Am. J. Hum. Genet. *87*, 110–114.
11. Fiscaletti, M., Biggin, A., Bennetts, B., Wong, K., Briody, J., Pacey, V., Birman, C., and Munns, C.F. (2018). Novel variant in Sp7/Osx associated with recessive osteogenesis imperfecta with bone fragility and hearing impairment. Bone *110*, 66–75.
12. Chen, J., Liu, C.-C., Li, Q., Nowak, C., Bu, G., and Wang, J. (2011). Two structural and functional domains of MESD required for proper folding and trafficking of LRP5/6. Structure *19*, 313–323.
13. Kubota, T., Michigami, T., and Ozono, K. (2009). Wnt signaling in bone metabolism. J. Bone Miner. Metab. *27*, 265–271.
14. Moosa, S., Yamamoto, G.L., Garbes, L., Keupp, K., Beleza-Meireles, A., Moreno, C.A., Valadares, E.R., de Sousa, S.B., Maia, S., Saraiva, J., et al. (2019). Autosomal-Recessive Mutations in MESD Cause Osteogenesis Imperfecta. Am. J. Hum. Genet. *105*, 836–843.

15. Stürznickel, J., Jähn-Rickert, K., Zustin, J., Hennig, F., Delsmann, M.M., Schoner, K., Rehder, H., Kreczy, A., Schinke, T., Amling, M., et al. (2021). Compound heterozygous frameshift mutations in MESD cause a lethal syndrome suggestive of osteogenesis imperfecta type XX. J. Bone Miner. Res *36*, 1077–1087.
16. Hsieh, J.-C., Lee, L., Zhang, L., Wefer, S., Brown, K., DeRossi, C., Wines, M.E., Rosenquist, T., and Holdener, B.C. (2003). Mesd encodes an LRP5/6 chaperone essential for specification of mouse embryonic polarity. Cell *112*, 355–367.
17. Gong, Y., Slee, R.B., Fukai, N., Rawadi, G., Roman-Roman, S., Reginato, A.M., Wang, H., Cundy, T., Glorieux, F.H., Lev, D., et al.; Osteoporosis-Pseudoglioma Syndrome Collaborative Group (2001). LDL receptor-related protein 5 (LRP5) affects bone accrual and eye development. Cell *107*, 513–523.
18. Boyden, L.M., Mao, J., Belsky, J., Mitzner, L., Farhi, A., Mitnick, M.A., Wu, D., Insogna, K., and Lifton, R.P. (2002). High bone density due to a mutation in LDL-receptor-related protein 5. N. Engl. J. Med. *346*, 1513–1521.
19. Little, R.D., Carulli, J.P., Del Mastro, R.G., Dupuis, J., Osborne, M., Folz, C., Manning, S.P., Swain, P.M., Zhao, S.C., Eustace, B., et al. (2002). A mutation in the LDL receptor-related protein 5 gene results in the autosomal dominant high-bone-mass trait. Am. J. Hum. Genet. *70*, 11–19.
20. Van Wesenbeeck, L., Cleiren, E., Gram, J., Beals, R.K., Bénichou, O., Scopelliti, D., Key, L., Renton, T., Bartels, C., Gong, Y., et al. (2003). Six novel missense mutations in the LDL receptor-related protein 5 (LRP5) gene in different conditions with an increased bone density. Am. J. Hum. Genet. *72*, 763–771.
21. Massink, M.P.G., Créton, M.A., Spanevello, F., Fennis, W.M.M., Cune, M.S., Savelberg, S.M.C., Nijman, I.J., Maurice, M.M., van den Boogaard, M.-J.H., and van Haaften, G. (2015). Loss-of-Function Mutations in the WNT Co-receptor LRP6 Cause Autosomal-Dominant Oligodontia. Am. J. Hum. Genet. *97*, 621–626.
22. Holdener, B.C., Faust, C., Rosenthal, N.S., and Magnuson, T. (1994). msd is required for mesoderm induction in mice. Development *120*, 1335–1346.
23. Liu, P., Wakamiya, M., Shea, M.J., Albrecht, U., Behringer, R.R., and Bradley, A. (1999). Requirement for Wnt3 in vertebrate axis formation. Nat. Genet. *22*, 361–365.
24. Guillemyn, B., Nampoothiri, S., Syx, D., Malfait, F., and Symoens, S. (2021). Loss of TANGO1 Leads to Absence of Bone Mineralization. JBMR Plus *5*, e10451.
25. Chang, W., Barnes, A.M., Cabral, W.A., Bodurtha, J.N., and Marini, J.C. (2010). Prolyl 3-hydroxylase 1 and CRTAP are mutually stabilizing in the endoplasmic reticulum collagen prolyl 3-hydroxylation complex. Hum. Mol. Genet. *19*, 223–234.
26. Takagi, M., Ishii, T., Barnes, A.M., Weis, M., Amano, N., Tanaka, M., Fukuzawa, R., Nishimura, G., Eyre, D.R., Marini, J.C., and Hasegawa, T. (2012). A novel mutation in LEPRE1 that eliminates only the KDEL ER- retrieval sequence causes non-lethal osteogenesis imperfecta. PLoS ONE *7*, e36809.

HGGA, Volume *2*

Supplemental information

Biallelic variants in *MESD*, which encodes a WNT-signaling-related protein, in four new families with recessively inherited osteogenesis imperfecta

Thao T. Tran, Rachel B. Keller, Brecht Guillemyn, Melanie Pepin, Jane E. Corteville, Samir Khatib, Mohammad-Sadegh Fallah, Sirous Zeinali, Fransiska Malfait, Sofie Symoens, Paul Coucke, Peter Witters, Elena Levtchenko, Hamideh Bagherian, Deborah A. Nickerson, Michael J. Bamshad, Jessica X. Chong, University of Washington Center for Mendelian Genomics, and Peter H. Byers

SUPPLEMENTARY MATERIAL & METHODS

Informed Consent: Written informed consent was obtained for all individuals in this study.

Exome filtering: In order to identify the causative gene in Family 1, we used the same WES data set described by Pyott *et al.*[5] which included five unrelated infants with OI phenotypes and the unaffected sibling of one of them. This data set was used to identify one of the first families in which *WNT1* [MIM 164820] pathogenic variants were shown to cause OI.[5] In all five families represented, the affected infant was from a recurrent sibling set. Four of the families were thought to be consanguineous and the fifth was from a defined ethnic community. In the included sibling pair, the affected child was found to be homozygous for a missense variant in *WNT1*. [5] Separately, another infant in the group was found to have a homozygous 20 kilobase deletion that encompassed exon 4 of *TMEM38B* [MIM 611236] and flanking splice sites. Prior to this analysis, the specific *TMEM38B* deletion had been described in other infants from the same population.[6] The exome sequence data had no coverage in the region of exon 4 of *TMEM38B*, which confirmed the deletion.

We took two approaches to the data analysis. The first was to repeat the method described by Pyott *et al* [5] using one of the unsolved infants from a consanguineous family in the previously described dataset (1-II:6) (Figure 3C) as the unknown. Briefly, we filtered the WES data for variants matching the expected homozygous recessive pattern of inheritance. We used the other three infants in the dataset (unaffected, *WNT1*, and*TMEM38B*) as "unaffected" controls and assumed that none of the remaining infants shared a causative variant. The analysis identified 55,915 variants from the reference exome seen in one or more of the individuals who were sequenced. We removed variants found in 1-II:6 that were also found in the other three individuals which left 9198 variants. Removal of intergenic

variants and those that appeared more than 10 times in the Exome Sequencing Project Exome Variant Server (EVS) left 936 variants. All heterozygous variants were discarded, as the family history suggested homozygous recessive inheritance, which left 123 variants. After intronic variants and synonymous coding variants were discarded, there were 62 candidates left. Those variants with a conservation score (consScoreGERP) >2 were discarded, leaving 24 variants. Of the 24, 11 genes were identified as potential candidates based on allele frequencies in the ExAC database (Supplemental Table 2).

For the second approach, the WES data were annotated with the Variant Effect Predictor v89[7] and analyzed with GEMINI 0.20.2.[7] We first checked for predicted pathogenic variants in all genes known to underlie OI.[2] We then focused on the same highly consanguineous family (Figure 2; Family 1), and filtered the WES data for variants that matched the expected homozygous recessive pattern of inheritance. Variants unlikely to impact protein-coding sequence (for which GEMINI impact_severity = LOW), variants filter flagged by the Genome Analysis Toolkit (GATK) as low quality (quality score ≤ 30, long homopolymer run > 5, low quality by depth < 5, within a cluster of SNPs), and variants with an alternative allele frequency >0.0005 in any superpopulation in gnomAD (v2.0), the Exome Variant Server (EVS), 1000 Genomes (phase 3 release), or >0.05 in an internal database of ~6400 individuals were excluded. Individual genotypes with depth < 6 or genotype quality < 20 were treated as missing in analysis. Due to the severity of OI in this family, we excluded all variants that were found in the homozygous state in the gnomAD database as gnomAD contains only putatively healthy adults. This yielded twenty candidate genes.

Genomic & cDNA Sequencing: DNA was extracted from patient fibroblasts or blood using the DNeasy Blood & Tissue Kit (Qiagen). RNA was extracted from patient fibroblasts using the RNeasy Mini Kit (Qiagen) and cDNA was generated with the Superscript First Strand

Synthesis System (Thermofisher Scientific). For confirmatory sequencing of *MESD*, exon 3 was amplified from either genomic DNA or cDNA using AmpliTaq Gold Polymerase (Applied Biosystems). The cycling program was: 95°C for 12 minutes, 95 °C for 10 seconds, 61 °C for 40 seconds, 72 °C for 50 seconds for 35 cycles, then, 72 °C for 7 minutes. Amplicons were treated with ExoSAP according to a standard protocol. Sequencing reactions were assembled using Big Dye v3.1 (Applied Biosystems) with the following program: 96°C for 10 seconds, 50 °C for 5 seconds, 60°C for 4 minutes for 40 cycles. Sequencing was run on an ABI 3730. Sequences were analyzed using Mutation Surveyor v5.0 (Softgenetics). Primers used for genomic and cDNA sequencing of MESD were as follows: MESD Genomic Sense 5'-TGCTCTGACCCCTTAGCACC-3', MESD Genomic Antisense 5'- GGGCAAAGAGCTCTCCACG-3', MESD cDNA Sense 5'- GTCGGGTAAGCGCGTCTAGG-3', and MESD cDNA Antisense 5'-AAGAGCTCTCCACGTCCACC-3'.

Immunoblotting: Protein lysates were prepared from primary fibroblasts using a buffer containing 0.05M Tris-HCl at pH 8.0, 0.15M NaCl, 5mM EDTA, 1% NP-40, and a protease inhibitor cocktail at 4 °C. 50µg of lysate was loaded per lane and resolved on a 10% SDS-PAGE gel in loading buffer containing 7.7 mg/ml dithiothreitol (DTT). Proteins were transferred to an Amersham Protran Premium 0.45□m Nitrocellulose Membrane (GE Healthcare). Detection for western blot was performed with primary antibodies for MESD (sc-139397; Santa Cruz Biotechnology, Inc.) at 1:00, LRP5 (sc-390267; Santa Cruz Biotechnology, Inc.) at 1:200, LRP6 (sc-25317; Santa Cruz Biotechnology, Inc.) at 1:300, and GAPDH (ab179811: Abcam) at 1:100. Detection was achieved using Amersham ECL Western Blotting Detection Reagent (GE Healthcare).

In Vitro Transcription/Translation (IVTT): In vitro transcription/translation (IVTT) was achieved using the 1-Step Human Coupled IVT Kit–DNA (ThermoFisher Scientific). Templates for IVTT were generated from an *MESD* cDNA expression plasmid (SC304244) from OriGene Technologies. Family-specific mutations were introduced into the *MESD* sequence using the QuikChange II Site-Directed Mutagenesis Kit (Agilent Technologies). Primers used for mutagenesis were:

QuikMESD_603- 606delTAAA_F 5'-
caaaggaggaggaagcaaagagaaaaaacaaagcaagacaa-3'; QuikMESD_603-
606delTAAA_R 5'- ttgtcttgctttgtttttttctctttgcttcctcctcctttg-3';
QuikMESD_632dupA_F 5'- caaagcaagacaagggcaaaaaaaaagaaggaaggagatct-3';
QuikMESD_632dupA_R 5'- agatctccttccttctttttttttgcccttgtcttgctttg-3';
QuikMESD_c676t_F 5'- ttattcccagctcaattttcttccttggaagaccgaga-3'; and
QuikMESD-c676t_R 5'- tctcggtcttccaaggaagaaaattgagctgggaataa-3'.

Fragments containing the cDNA sequence with upstream T7 promotors were liberated using Sac-I (New England BioLabs) and gel purified using the QIAquick Gel Extraction Kit (Qiagen). Approximately 125ng of linearized template was used in IVTT reactions that were incubated for 6 hours at 30°C. 2microliters of each IVT reaction was run on a 10% SDS-PAGE gel in loading buffer containing 7.7 mg/ml dithiothreitol (DTT). Western Blot was performed using primary antibody against MESD (sc-139397; Santa Cruz Biotechnology, Inc.) at 1:100 followed by HRP-Conjugated Goat Anti-Rabbit IgH H&L (ab6721; Abcam) secondary antibody at 1:20,000. Detection was achieved using Amersham ECL Western Blotting Detection Reagent (GE Healthcare).

Immunocytochemistry (ICC): Primary dermal fibroblasts from I-II:6 and from a control patient (A8) cultured in DMEM 10% FBS were fixed in cold methanol for 10 minutes and incubated with 2.5% normal horse serum/PBS (Vector Laboratories) for 20 minutes at room temperature to block nonspecific binding of antibodies. The cells were incubated with primary antibody to MESD (sc-139397; Santa Cruz Biotechnology, Inc.) at 1/50 at 4°C overnight. This was followed by incubation with AlexaFluor488 Goat Anti-Rabbit IgH (H&L) (A11034; ThermoFisher Scientific), 1:500, at room temperature for 1 hour. This stepwise staining process was repeated for KDEL (ab176333; Abcam) at 1:100 with AlexaFluor594 Goat Anti-Rabbit IgH (H&L) (A11037; ThermoFisher Scientific) at 1:800. The cells were counterstained with DAPI and mounted on slides. Images were acquired with a Zeiss Imager A1.

SUPPLEMENTARY TABLES AND FIGURES

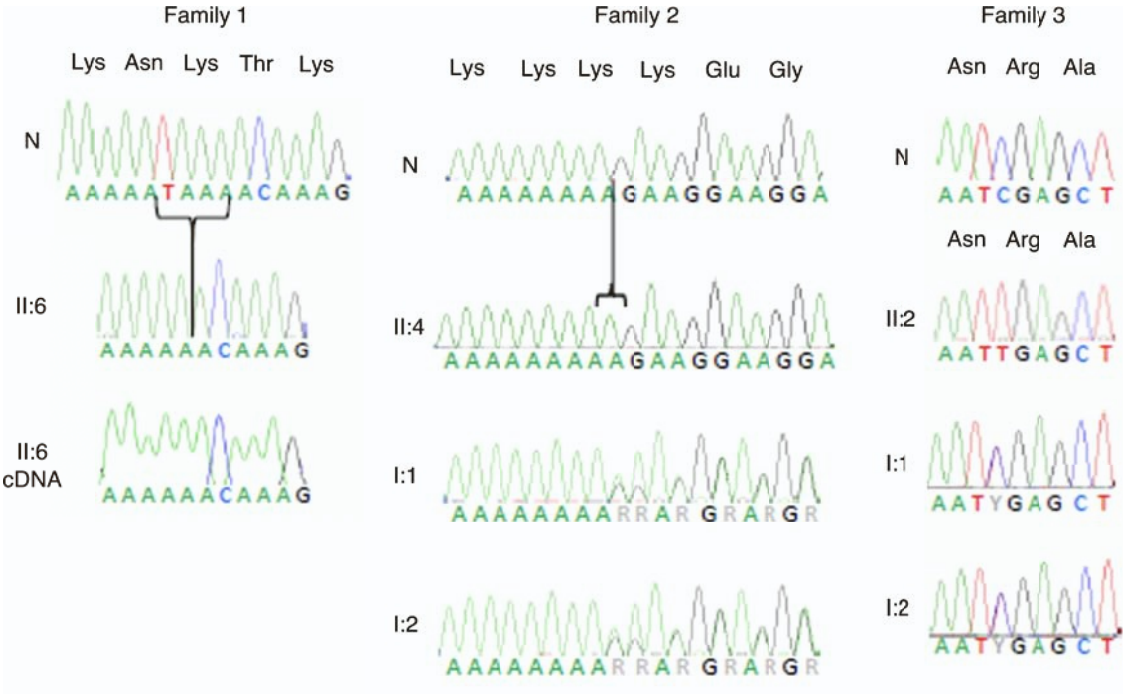

Supplemental Figure 1. MESD confirmational sequencing. Variant sequences from available family members confirming the homozygous small deletion (c.603-606delTAAA) in Family 1 (both in proband genomic DNA and cDNA), the duplication (c.632dupA) in Family 2 (in the homozygous proband and in both heterozygous parents), and the substitution mutation (c.676C>T) in Family 3 (in the homozygous proband and in both heterozygous parents)(the proband in Family 4 carries the same homozygous mutation). The normal reference sequence sequences are labeled 'N'.

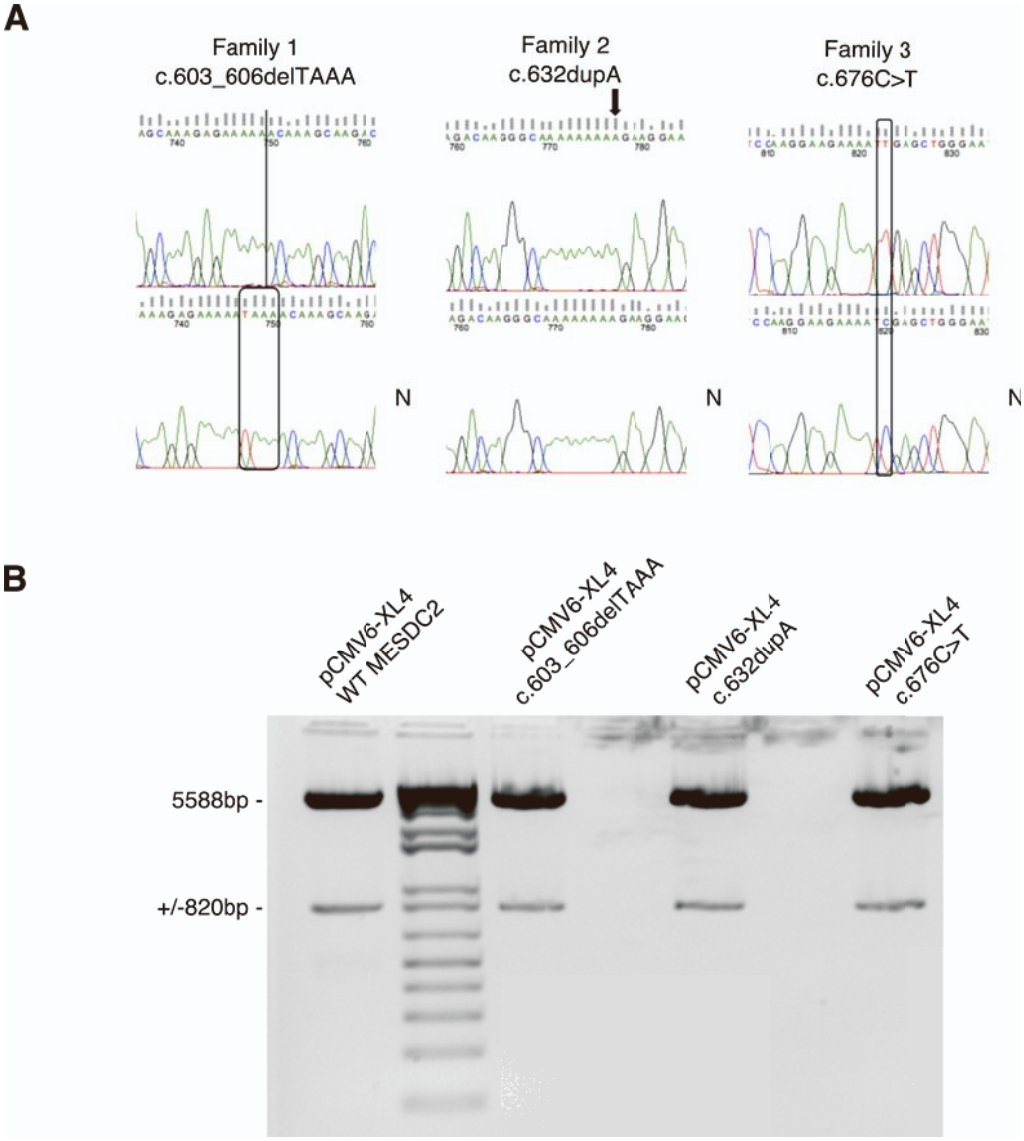

Supplemental Figure 2. IVTT DNA Templates. (A) Mutagenesis introducing family variants in MESD was confirmed by Sanger sequencing. The normal reference sequences are labeled 'N'. (B) Sac-I digestion of T7-MESD cDNA fragments away from pCMV6-XL4 expression plasmid backbone.

Supplemental Table 1: Genes associated with OI.

Gene Name	MIM
COL1A1	MIM 120150
COL1A2	MIM 120160
IFITM5	MIM 614757
BMP1	MIM 112264
CREB3L1	MIM 616215
CRTAP	MIM 605497
FKBP10	MIM 607063
MBTPS2	MIM 300294
P3H1	MIM 610339
PLOD2	MIM 301865
PPIB	MIM 123841
SEC24D	MIM 607186
SERPINF1	MIM 172860
SERPINH1	MIM 600943
SP7	MIM 606633
SPARC	MIM 182120
TENT5A	MIM 611357
TMEM38B	MIM 611236
WNT1	MIM 164820
MESD	MIM 618644
CCDC134	?
KDELR2	MIM619131

Supplemental Table 2. Candidate Genes From Exome Analysis. N/A = not available.

Chromosomal Location	Gene	Protein	Coding Change	Protein Change	Alteration	Clinical Associations
Chromosome 1: 66,533,383-66,748,299	*SGIP1* MIM 611540	SH3-Domain GRB2-Like (Endophilin)-Interacting Protein 1 (SGIP1)	c.1199C>A	p.Pro400His	missense	N/A
Chromosome 1: 205,042,937-205,078,499	*CNTN2* MIM 190197	Contactin 2 (CNTN2)	c.2377C>T	p.Arg793Cys	missense	epilepsy [28]
Chromosome 3: 126,006,355-126,101,561	*SLC41A3* MIM 610803	Solute Carrier Family 41, Member 3 (SLC41A3)	c.533G>A	p.Ile178Thr	missense	N/A

Chromosome 12: 6,693,792-6,700,800	*PIANP* MIM 616065	PILR-Alpha-Associated Neural Protein (PANP)	c.214G>A	p.Arg72Trp	missense	immune regulation (*m. musculus)* [29]
Chromosome 13: 96,090,839-96,839,562	*HS6ST3* MIM 609401	Heparin Sulfate 6-O-Sulfotransferase 3 (HS6ST3)	c.688C>T	p.Arg230Cys	missense	N/A
Chromosome 14: 57,200,507-57,269,008	*EXOC5* MIM 604469	SEC10-Like 1 (SEC10L1)	c.2074C>T	p.Val692Ile	missense	N/A
Chromosome 15: 80,946,289-	*MESD* MIM 607783	Mesoderm Development Gene (MESD)	c.603-606delTAA	p.Asn201Lysfs *15	frameshift	failure to form mesoderm, patterning defects, embryonic lethality (*m. musculus*) [9; 14]

80,989,878

Chromosome 17: 7,839,904-7,854,796	*KDM6B* MIM 611577	Jumonji Domain-Containing Protein 3 (JMJD3)	c.1825G>A	p.Ala609Thr	missense	Mental Retardation, Autosomal Recessive 33 [MIM 614341] (not confirmed) [30; 31]
Chromosome 19: 11,834,341-11,419,342	*RGL3* MIM 616473	Ral Guanine Nucleotide Dissociation Stimulator-Like 3 (RGL3)	c.1046G>T	p.Ala349Asp	missense	N/A
Chromosome 19: 49,766,968-49,807,113	*AP2A1* MIM 601026	Clathrin Adaptor Complex AP2, Alpha Subunit (AP2-Alpha)	c.2063G>T	p.Gly688Val	missense	N/A